ELSEVIER

Contents lists available at ScienceDirect

Carbohydrate Polymers

journal homepage: www.elsevier.com/locate/carbpol



Investigation of composition, structure and bioactivity of extracellular polymeric substances from original and stress-induced strains of *Thraustochytrium striatum*



Rui Xiao^a, Xi Yang^b, Mi Li^c, Xiang Li^a, Yanzhang Wei^b, Min Cao^d, Arthur Ragauskas^{c,e,f}, Mark Thies^g, Junhuan Ding^g, Yi Zheng^{a,*}

- ^a Department of Environmental Engineering and Earth Sciences, Clemson University, 342 Computer Court, Anderson, SC 29625, USA
- ^b Department of Biological Sciences, Life Sciences Facility, Clemson University, Clemson, SC 29634, USA
- ^c Joint Institute of Biological Science, Biosciences Division, Oak Ridge National Laboratory, Oak Ridge, TN 37831, USA
- ^d Department of Biological Sciences, 132 Long Hall, Clemson University, Clemson, SC 29634, USA
- ^e Department of Chemical and Biomolecular Engineering, University of Tennessee, Knoxville, TN 37996, USA
- Department of Forestry, Wildlife, and Fisheries, Center for Renewable Carbon, University of Tennessee Institute of Agriculture, Knoxville, TN 37996, USA
- ⁸ Department of Chemical and Biomolecular Engineering, Clemson University, Clemson, SC 29634-0909, USA

ARTICLE INFO

Keywords: Thraustochytrium striatum Marine protist Extracellular polymeric substances Exopolysaccharide Bioactivity Nitrogen stress

ABSTRACT

This paper was the first to study extracellular polymeric substances (EPSs) of *Thraustochytrium striatum* on composition, structure and bioactivities. Two strains of *T. striatum* including original (ori) and high-biomass (mut) strains (induced by high-nitrogen stress) were compared. The EPSs from both strains mainly contained polysaccharide (41–64%, w/w, dry basis) and protein (25–40%, w/w, dry basis), which was shown by the morphology study with an AFM. The monosaccharide profile of the EPS polysaccharide was consisted of glucose, galactose, arabinose, and trace amount of xylose. Glucose and arabinose took up to 82–90% (w/w, dry basis) of the total polysaccharide. The structure and functional groups of EPSs were determined by FTIR and NMR. The NMR results revealed that the major structural linkages of the polysaccharides of both ori and mut EPSs were $1 \rightarrow 6$ - β -glucan and $1 \rightarrow 4$ - α -galactan branched with 1- α -arabinose. The EPSs were found to have anti-tumor activities against mouse melanoma B16-F0, human prostate carcinoma DU145, human cervical carcinoma HeLa, and human lung carcinoma A549. The EPSs also showed antioxidant and anti-inflammatory activities and antibacterial activity against *Pseudomonas aeruginosa*.

1. Introduction

Many microorganisms can excrete extracellular polymeric substances (EPSs) into their immediate environment during their metabolism. Generally, the EPSs have been observed in bacteria (including cyanobacteria), Cryptophyta, mushroom, yeast, basidiomycete, and protist (Jain, Raghukumar, Tharanathan, & Bhosle, 2005; Mishra & Jha, 2009). The EPSs are composed of a complex high-molecular-weight mixture of biopolymers, such as polysaccharides, proteins, nucleic acids, and lipids. They can hold microbial cells together to form a heterogeneous matrix and affect the physicochemical properties of cell aggregates, including flocculation, structure, surface charge, viscosity, and settling properties (Flemming & Wingender, 2010; Xiao & Zheng, 2016). The EPSs are versatile, natural biopolymers that can function as anticoagulants to protect the host cells against dewatering and toxic

substances, and that can serve as extracellular carbon and energy sinks in response to environmental stress (Xiao & Zheng, 2016).

In addition to the role in the metabolism of host cells, the EPSs also represent a biotechnologically important class of renewable source of structurally and compositionally diverse biopolymers that possess unique bioactivities for potential high-value biological applications, including antivirals, anti-tumor agents, antioxidants, anticoagulants, antibacteria, and anti-inflammatories (de Jesus Raposo, de Morais, & de Morais, 2015a). In recent years, interest in the EPSs has been increasing for various industrial applications, such as detoxification of heavy metals and radionuclides from contaminated water, removal of solid matter from water reservoirs, and improvement of soil water holding capacity (Bender & Phillips, 2004). The superior rheological properties make the EPSs particularly useful in food science/engineering (e.g., thickener and preservatives) and mechanical engineering (e.g.,

E-mail address: zheng9@clemson.edu (Y. Zheng).

^{*} Corresponding author.

biolubricants and drag reducers) (Arad & Atar, 2015; Arad et al., 2006; Gasljevic, Hall, Chapman, & Matthys, 2008; Ha, Dyck, & Thomas, 1988; Yaron, Cohen, & Arad, 1992).

Extensive research has been focused on the EPSs from bacteria and microalgae, and EPSs that have been applied at industrial scale are mainly obtained from bacteria including cyanobacteria. However, the increased demand for natural polymers has resulted in growing interest in exploiting new EPS sources. Thraustochytrids are one group of marine microorganisms that are an extremely common component of microbial consortia in the sea, and their biomass production capability is comparable to that of bacteria (Jain et al., 2005). They are a diverse group of heterotrophic, obligate marine protists, and they have been found in microbial films on submerged surfaces in the sea (Raghukumar, 2002: Raghukumar, Anil, Khandeparker, & Patil, 2000). Due to their abundance in the marine environment, it is of intrinsic interest to investigate the applications of Thraustochytrids from the perspective of their biotechnological importance in addition to their ecological role. Thraustochytrids have been the subject of recent studies in that they can produce nutraceuticals (e.g., docosahexaenoic acid-DHA, eicosapentaenoic acid-EPA, and astaxanthin) and lipids [e.g., palmitoleic acid (C16:1) and oleic acid (C18:1)] for biodiesel production (Aki et al., 2003; Burja, Armenta, Radianingtyas, & Barrow, 2007; Byreddy, Gupta, Barrow, & Puri, 2015; Byreddy, 2016; Carmona, Naganuma, & Yamaoka, 2003; Singh et al., 2015). However, very limited studies reported the production and characterization of EPSs from these protists (Jain et al., 2005; Lee Chang et al., 2014; Liu, Singh, Sun, Luan, & Wang, 2014).

This research was focused on a Thraustochytrid strain of T. striatum of which EPSs have never been studied. T. striatum is a unicellular, eukaryotic, chemo-organotrophic, and marine stramenopilan protist (Bongiorni, Jain, Raghukumar, & Aggarwal, 2005). It has been found in various habitats, such as plant detritus (e.g., mangrove and brown algae), fecal pellets of zooplankton, rocky shores, salt marshes, and coastal waters, but rarely found on living plants (Raghukumar, Sharma, Raghukumar, Sathe-Pathak, & Chandramohan, 1994; Raghukumar, Sathe-Pathak, Sharma, & Raghukumar, 1995; Raghukumar & Raghukumar, 1999). T. striatum demonstrated a dual role in nature, namely a fungus-like breakdown and mineralization of highly refractory organic matter in marine ecosystems as well as bacterivory by means of extracellular enzyme system (Raghukumar, 1992). Its cell walls are multilamellate, made up of dictyosome-derived circular scales comprising sulphated polysaccharides, instead of chitin microfibrils found in fungus cell walls (Bongiorni et al., 2005). Its sporangial wall fragments at maturity to release the zoospores in a non-proliferous form (Harrison & Jones, 1974). To adapt to its complex habitats, T. striatum is able to withstand the fluctuations of environmental conditions, such as pH, temperature, and salinity (Fan, Vrijmoed, & Jones, 2002). It was found to be able to use a wide spectrum of carbon sources, e.g., starch, pectin, chitin, lignocellulose, etc. (Taoka et al., 2009). The objectives of this work are to: (1) examine the production and composition of the EPSs from T. striatum; (2) characterize the chemical structure of the EPSs; and (3) study the bioactivities of the EPSs including anti-tumor, antioxidant, anti-inflammatory, and antibacterial activities. The present research also involved the effect of culture growth condition (i.e., MgSO₄ concentration) on the production, characterization and bioactivity of EPSs, and the dose-dependency of EPS bioactivity was determined as well.

2. Materials and methods

2.1. Protist culture preparation

The EPSs in this research were produced by *T. striatum* ATCC 24473 that was purchased from ATCC. The culture was prepared by following the guidelines provided by ATCC. Briefly, *T. striatum* culture was grown in a glucose-yeast extract-peptone (GYP) medium prepared in 100% artificial seawater (ASW) at 25 °C and pH 7.0 in the dark with the

agitation speed of 150 rpm. The GYP medium contained 30 g/L of glucose, 6 g/L of yeast extract and 6 g/L of peptone. The ASW was prepared by dissolving the following salts in deionized distilled water (per liter): 30 g of NaCl, 0.7 g of KCl, 10.8 g of MgCl₂·6H₂O, 5.4 g of MgSO₄·7H₂O, and 1.0 g of CaCl₂·2H₂O (Nagano, Taoka, Honda, & Hayashi, 2009). Since the increased sulfur content of EPSs was reported to correlate with enhanced bioactivity (de Jesus Raposo, de Morais, & de Morais, 2015b), we tried to increase the sulfur content of the EPSs for achieving higher bioactivity by increasing MgSO₄·7H₂O concentration to 10.8 and 16.2 g/L in the GYP medium (Xiao & Zheng, 2016). In this research, two strains of T. striatum were used to produce EPSs. The one was the original strain from ATCC, and the other was a high-biomass strain induced by nitrogen stress that was created by incubating the original strain at high nitrogen concentration of 20 g/L (10 g/L of yeast extract and peptone each) for ten generations. The high-biomass strain has much higher biomass yield, substrate utilization efficiency and EPS yield than the original strain. To produce EPSs, both strains were cultivated under the same aforementioned cultivation conditions for comparison. In this paper, we use "ori" and "mut" to represent the original and high-biomass strains, respectively unless specified, otherwise.

2.2. Preparation of EPSs

When *T. striatum* culture reached the late stationary phase in 7 days (turning point to death phase), the culture was harvested and centrifuged at 4000 rpm for 5 min at 4 °C. The pellet was discarded, and the supernatant was first filtered through a 0.45- μ m filter paper. The filtrate was then concentrated about ten times (i.e., volume reduction from 150 to 15 mL) in an Amicon* stirred cell by ultrafiltration (UF) through a PES membrane (Sterlitech, Kent) with a molecular weight cutoff (MWCO) of 10 kDa. To further purify the EPSs, about 100 mL deionized distilled (DDI) water was added to the concentrated EPSs in the UF cell and the mixture was dialyzed against DDI water until negligible conductivity (Hach SC200 Universal Controller, Hach, CO, USA) change was found in the permeate, during which permeate was removed periodically. At last, the purified concentrated EPSs in the retained solution were harvested and lyophilized and stored at -20 °C until used (Jain et al., 2005).

2.3. Characterization of EPSs

Total carbohydrate was determined by using phenol-sulfuric acid method with glucose as a standard (Masuko et al., 2005). The protein content of EPSs was determined by using Pierce™ Modified Lowry Protein Assay Kit (ThermoFisher Scientific). Uronic acid of the EPSs was measured according to the method used by Mojica et al. (2007). The sulfate content of EPSs was quantified by modifying the method developed by Dodgson (1961). Initially, 20 mg of EPS sample was hydrolyzed by 3 mL of 60% formic acid (v/v) for 8 h under 100 $^{\circ}$ C, and the hydrolysate was collected for sulfate content measurement by using colorimetric method. The color development resulted from the reaction between sulfate and the gelatin-BaCl₂ reagent. To prepare the reagent, 2 g of gelatin was dissolved in 400 mL of DDI water at 60 °C and stood at 4°C overnight followed by dissolving 2 g of BaCl2 into the gelatin solution and holding for 3 h prior to use. During the sulfate analysis, $500\,\mu L$ of sulfate samples were mixed with $3.8\,mL$ of trichloroacetic acid (TCA) (4%, w/v) and 1 mL of gelatin-BaCl2 reagent for 15 min for color development. The absorbance was measured at $\lambda = 500\,\text{nm}$. Potassium sulfate was used as a standard with the concentration in the range of 0–100 μ g SO_4^{2-}/mL .

To analyze the compositional monosaccharides, lyophilized EPSs of 5–10 mg were hydrolyzed with 2 M $\rm H_2SO_4$ for 5 h at 121 °C (Mishra & Jha, 2009). After complete hydrolysis, content was neutralized by using CaCO $_3$ to pH 7.0 and filtered into HPLC vials through 0.2- μ m syringe filters. Monosaccharide composition of the hydrolysate was measured

by HPLC (Sluiter et al., 2008) (Dionex UltiMate 3000, Thermo Scientific) equipped with a refractive index (RI) detector (Shodex RI-101, Showa Denko America) and a Shodex carbohydrate analytical column (Sugar SP0810, Showa Denko America). The separation temperature was 85 °C, and HPLC grade water was used as mobile phase at a flow rate of 0.6 mL/min. A deashing guard column (Shodex Sugar SP-G 6B, Showa Denko America) was installed prior to the analytical column to prevent column contamination.

The lipid was measured as the sum of fatty acid methyl esters (FAMEs) which was determined using the direct transesterification method (Burja, Radianingtyas, Windust, & Barrow, 2006). The GC (Shimadzu GC-2010) had a flame ionization detector (FID) and a FAME analytical column (Rt-2560, Restek). The carrier gas was helium. The temperature for both injector and detector was 240 °C. The programmed temperature for the column oven started from 100 °C held for 5 min and increased to 240 °C with the ramp rate of 4 °C/min. Supelco° 37 component FAME mix was used as the FAME standard (Sigam-Aldrich, U.S.A) with methyl tridecanoate (200 $\mu g/mL$) as an internal standard for recovery correction.

The molecular weights of the EPSs were determined by gel permeation chromatography (GPC) (Alliance GPCV 2000, Waters). Two analytical columns were used in series, i.e., a Waters Styragel $^{^{\circ}}$ HT5 column followed by an Agilent PolarGel-L column. The mobile phase was 0.05 M lithium bromide in N, N-dimethylformamide at a flow rate of 1 mL/min. Poly-(ethylene glycol) (PEG) was used as a calibration standard for determination of the number average (Mn) and the weight average (Mw) molecular weights. The polydispersity index (PDI) was equal to the ratio of $M_{\rm w}/M_{\rm n}$. Prior to GPC analysis, EPS samples were dissolved in the mobile phase at a concentration of 1 mg/mL and filtered through 0.2-µm nylon-membrane filter. The signals were detected by a Waters 2414 refractive index detector.

Fourier transform infrared (FTIR) spectroscopy was performed using an instrument (Thermo Nicolet 6700 spectrometer, Thermo Scientific) equipped with a single bound diamond attenuated total reflectance (ATR) cell (Smart iTR, Thermo Scientific) at room temperature. Around 2 mg of freeze-dried EPS powder (obtained at 5.4 g/L of MgSO₄·7H₂O) was deposited on the diamond platform and dried further by air prior to measurement. Background and sample spectra were acquired at 4 cm $^{-1}$ resolution with 64 scans from 600 to 4000 cm $^{-1}$.

NMR spectra were recorded at 30 °C on a Bruker Avance III HD 500 spectrometer, and spectral processing was carried out using a Bruker Topspin 3.5 (Mac) software. The EPS samples (50 mg obtained at 5.4 g/ L of MgSO₄·7H₂O) were dissolved in D₂O (99.9%) for deuterium exchange before freeze-drying. The lyophilized sample was then dissolved in $0.5\,\text{mL}$ D₂O (99.9%) for data acquisition in 5 mm NMR tube. The ^1H and ^{13}C NMR spectra were recorded at 500 MHz and 125.75 MHz cryoprobe (BBO 1H & 19F-5mm), respectively. The 2D heteronuclear single quantum coherence (HSQC) NMR experiments were conducted with a standard Bruker pulse sequence (hsqcetgpspsi2.2) using the following acquisition parameters: spectra width 12 ppm in F2 (1H) dimension with 1024 data points (acquisition time 85.2 ms), 166 ppm in F1 (¹³C) dimension with 256 increments (acquisition time 6.1 ms), a 1.0-s delay, a $^1J_{\text{C-H}}$ of 145 Hz, and 128 scans. Acetone ($\delta_H = 2.23 \text{ ppm}$ and $\delta_C = 30.89$ ppm) were used as internal calibration standards for ¹H, ¹³C and HSOC NMR chemical shifts. The peaks were assigned according to the literature (Gharzouli, Carpéné, Couderc, Benguedouar, & Poinsot, 2013; Lowman et al., 2011; Nie, Liu, She, Sun, & Xu, 2013).

2.4. EPS bioactivity assay

2.4.1. Anti-tumor activity analysis

2.4.1.1. Cancer cell preparation. Mouse melanoma B16-F0 cells, human prostate carcinoma DU145 cells, and human cervical carcinoma HeLa cells were cultivated in DMEM (Dulbecco's Modified Eagle Medium) high glucose cell culture medium containing 10% fetal bovine serum and $100\,\mu\text{g/mL}$ gentamicin. Human lung epithelial NL20 cells were

cultivated in Ham's F12 medium which contained 1.5 g/L of sodium bicarbonate, 2.7 g/L of glucose, 2.0 mM of L-glutamine, 0.1 mM of nonessential amino acids, 0.005 mg/mL of insulin, 10 ng/mL of epidermal growth factor, 0.001 mg/mL of transferrin, 500 ng/mL of hydrocortisone, and 10% fetal bovine serum. Human lung carcinoma A549 cells were cultivated in F-12K medium containing 10% fetal bovine serum and 100 $\mu g/mL$ of gentamicin. All cancer cells were incubated at 37 °C with the aeration of 5% CO $_2$ unless specified, otherwise.

2.4.1.2. Cell cytotoxicity assay. Cells in triplicates were cultivated in 96-well plates for 24 h to achieve a density of 10,000 cells per well. Once ready, cells were incubated with varying concentrations of EPS samples $(0.1-100\,\mu g/mL)$ in cell culture medium for another 48 h. The blank controls without EPS addition were also conducted for comparison. Cell death was then measured using CellTiter 96 AQueous non-radioactive cell proliferation assay (Promega, Madison, WI) by following manufacturer's directions. The absorbance spectra (λ = 490 nm) were collected using a microplate reader (BioTek Eon, BioTek, Winooski, VT) equipped with Gen5 All-in-One data analysis software.

2.4.2. Total antioxidant capacity

The total antioxidant capacity (TAC) of EPS samples with varying concentrations (10, 30 and 100 $\mu g/mL)$ was determined with the QuantiChrom $^{\text{\tiny IM}}$ Antioxidant Assay Kit (BioAssay Systems, CA, USA) by following manufacturer's instructions. TAC of each EPS sample was calculated and expressed as μM trolox equivalents against a trolox standard curve.

2.4.3. Anti-inflammatory activity

Mouse macrophage Raw 264.7 cells were cultivated in DMEM high glucose cell culture medium containing 10% fetal bovine serum and 100 ug/mL of gentamicin, Lipopolysaccharide (LPS) (Sigma Aldrich, U.S.A) was solubilized in sterile DDI water to make the stock solution at a concentration of 1 mg/mL. To do the test, Raw 264.7 cells were cultivated in 96-well plates for 24 h, and LPS was added to the cell cultures at a concentration of 0.5 µg/mL to induce inflammation. After 24-h incubation, EPS samples with varying concentrations (10, 30 and 100 µg/mL) were added to cell cultures followed by overnight incubation. Here, two controls were also conducted in parallel including a blank control (cell cultures without LPS or EPSs) and a LPS control (cell cultures with LPS but without EPSs). The mixtures were centrifuged and the supernatant from each treatment was collected for anti-inflammation activity measurement using Griess Reagent Kit for Nitrite Determination (Molecular Probes) with a microplate reader $(\lambda = 548 \text{ nm})$ (BioTek Eon, BioTek, Winooski, VT) by following the manufacturer's directions. To distinguish the potential decrease of nitric oxide (NO) production caused by EPS-induced macrophage cell death, the cell proliferation assay was also performed according to the method in Section 2.4.1.

2.4.4. Antibacterial activity

The bacterial strains used in this study were *Enterococcus faecalis* ATCC 47077, *Listeria monocytogenes* 10403S serotype 1/2a, *Staphylococcus aureus* ATCC 25923, *Escherichia coli* 0157:H7 ATCC700927, *Pseudomonas aeruginosa* ATCC 27853, *Salmonella enterica* ATCC 29631, and *Vibrio cholerae* C6706 (O1 El Tor). *E. faecalis, L. monocytogenes, S. aureus*, and *S. enterica* were cultured in Brain-heart infusion medium (BHI). *E. coli* 0157:H7, *P. aeruginosa* and *V. cholerae* C6706 were cultured in Lysogeny Broth (LB). The EPS samples used in this section for antibacterial analysis were obtained from the cultures of both original and high-biomass strains cultivated with 5.4 g/L of MgSO₄·7H₂O in the GYP medium.

2.4.4.1. Zone of inhibition (ZOI) assay. The tested bacteria were grown in either LB or BHI medium overnight at 37 $^{\circ}$ C. The overnight cultures

were 1:100 diluted into fresh medium and incubated until reaching mid-log stage. A 100- μL of the cell culture was mixed with 3 mL of 0.7% soft LB or BHI agar and poured onto the bottom agar in a petri dish. When the top agar was solidified, a piece of filter disc ($\Phi=6$ mm) was placed on the top of the agar, and $10\,\mu L$ of EPSs (1, 10, 20, and 50 mg/ mL) was dropped onto the filter disc. The petri dishes were incubated overnight at 37 °C and were observed the next day. A clear zone around the filter disc indicated the growth inhibition of the tested bacteria.

2.4.4.2. Minimal inhibitory concentration (MIC) assay. Since only *P. aeruginosa* was found sensitive to the EPS samples in the ZOI test, it was selected for MIC assay. Overnight *P. aeruginosa* culture was 1:100 diluted into fresh LB medium with increasing concentrations of EPSs (0, 78, 156, 312.5, 625, 1250, 2500, 5000, and 10,000 µg/mL). The growth of each culture was observed after overnight incubation at 37 °C with shaking at 100 rpm. The bacterial growth was detected by optical density (OD) at $\lambda = 600$ nm.

2.5. Data analysis

All measurements were implemented in triplicate unless specified, otherwise. Statistical differences were determined using one way ANOVA with Tukey's post-test using Graphpad Prism software (GraphPad Software Inc., CA). Statistical differences were represented as ***p < 0.001, **p < 0.01 and *p < 0.05.

3. Results and discussion

3.1. Compositional characteristics of EPSs

The protist cultures showed characteristic sigmoidal growth curves while EPS production was observed at all stages of growth and the concentration increased with age (Data not shown), reaching the maximum values at the 7th day of cultivation during the stationary phase. The EPSs were visualized with atomic force microscopy (AFM) imaging technique (Fig. S1). We speculate that the high level of EPS accumulation in the later developmental stages provides an important substrate for the heterotrophic protist. For both ori and mut strains, the increasing MgSO₄ concentration in the medium was a highly effective method to enhance the EPS production, i.e., the EPS concentration was increased by 45 and 15% for ori and mut strains, respectively with the increase of MgSO₄·7H₂O concentration from 5.4 to 16.2 g/L (Table 1). Compared to the ori strain, the mut strain achieved much higher EPS concentration. Especially, the lowest EPS concentration (1825.5 mg/L)

for the mut strain with 5.4 g/L of MgSO₄·7H₂O was still higher than the highest EPS concentration (1004.5 mg/L) for the ori strain with 16.2 g/ L MgSO₄·7H₂O, which indicates that nitrogen stress can stimulate the EPS production. Therefore, both nitrogen stress and increasing MgSO₄ concentration could be used to optimize EPS production in future research. Compared to other Thraustochytrid protists (Schizochytrium sp. and Thraustochytrium sp.) reported by Jain et al. (2005), the EPS vield of the ori strain in our study is similar to that of different species of Thraustochytrium genus, but lower than that of the strains of Schizochytrium genus. However, the mut strain produced much higher EPSs than the strains of both genera Thraustochytrium and Schizochytrium. It should be aware that we have not attempted to optimize EPS production even though the EPS vield in this study is far lower than that of some bacteria. For instance, Xanthomonas species and cyanothece sp. 113 can produce 33 and 22 g/L of EPSs, respectively (Chi, Su, & Lu, 2007; Sutherland, 1998). It is likely that T. striatum in our study would produce larger amount of EPSs under optimal conditions.

In the characterization of EPSs, we analyzed total carbohydrate, protein, uronic acid, and sulfate, and lipid that are commonly present in EPSs from other organisms (e.g., bacteria and microalgae) (Xiao & Zheng, 2016). As shown in Table 1, carbohydrate and protein contents took up about 80-90% of the EPSs from both ori and mut strains. Overall, increasing MgSO₄ concentration reduced carbohydrate content, but raised other components. Compared with the ori strain, the mut strain had much lower protein content in its EPSs while its carbohydrate content was much higher (Fig. S1), which implies that nitrogen stress can induce carbohydrate synthesis while suppressing protein formation in the EPSs of T. striatum. This mechanism may be used by T. striatum to balance the C/N ratio of the EPSs in response to the nitrogen stress because EPSs can serve as carbon and energy sources for cell growth under stress, which needs to be further studied, e.g., genome sequencing to distinguish if nitrogen stress causes mutations or gene expression change of T. striatum.

It was revealed that sulfate and uronic acid conferred an overall negative charge and acidic property to the EPSs (Geresh, Arad, & Shefer, 1997; Geresh, Dubinsky, Arad, Christiaen, & Glaser, 1990). Hydrated sulfated polysaccharides are known to be able to retain moisture and protect host cells from desiccation (Decho, 1990). Such EPSs produced by *T. striatum* could help prevent cells from dehydration. Sulfated polysaccharides from other microorganisms such as cyanobacteria (e.g., *Aphanocapsa halophytia*) and red alga (e.g., *Porphyridium cruentum*) are also of biotechnological importance (e.g., anti-inflammatory, antimicrobial, blood anticoagulants, and antivirus) (de Jesus Raposo, de Morais, & de Morais, 2013; Fabregas et al., 1999;

Table 1
Chemical compositions and molecular weights of EPSs from ori and mut strains of *T. striatum* under different MgSO₄·7H₂O concentrations in GYP medium.

Category	Component	MgSO ₄ ·7H ₂ O co	oncentration (g/I	centration (g/L)				
		Ori strain		Mut strain				
		5.4	10.8	16.2	5.4	10.8	16.2	
Total EPSs (mg/L)	Concentration	692.5 ± 17.7	905.0 ± 31.1	1004.5 ± 21.9	1825.5 ± 43.1	2042.5 ± 39.6	2107.3 ± 24.0	
Composition of EPSs (wt%, dry basis)	Carbohydrate Protein Uronic acid Sulfate content Lipid	47.0 ± 1.4 37.4 ± 0.2 6.2 ± 0.6 6.4 ± 0.4 1.0 ± 0.0	44.8 ± 0.2 39.9 ± 0.6 8.9 ± 0.7 8.6 ± 0.3 0.8 ± 0.0	40.5 ± 0.3 40.3 ± 3.4 13.2 ± 0.6 9.6 ± 0.7 1.4 ± 0.2	64.1 ± 1.1 25.0 ± 1.1 3.4 ± 0.6 5.2 ± 0.5 0.7 ± 0.0	59.0 ± 1.4 28.1 ± 1.4 7.7 ± 0.2 5.2 ± 0.1 0.3 ± 0.0	55.4 ± 1.3 26.5 ± 0.6 10.7 ± 0.2 6.6 ± 1.1 0.4 ± 0.0	
Monosaccharide content of EPS carbohydrate (wt%, dry basis)	Glucose Xylose Galactose Arabinose	43.2 ± 1.4 2.8 ± 0.9 14.5 ± 0.3 39.4 ± 0.8	36.5 ± 0.5 5.6 ± 0.8 11.1 ± 0.4 46.7 ± 0.0	45.0 ± 1.3 14.6 ± 1.1 ND 40.4 ± 0.1	11.5 ± 0.2 ND 8.3 ± 0.2 81.2 ± 0.0	11.8 ± 0.1 2.5 ± 0.1 8.3 ± 0.5 77.3 ± 0.2	19.8 ± 1.8 7.6 ± 0.6 11.4 ± 1.8 61.2 ± 3.0	
Molecular weight (kDa) and PDI of EPSs	M _w PDI	375 3.58	367 8.22	374 5.38	160 4.41	414 7.49	398 7.90	

Guzmán, Gato, Lamela, Freire-Garabal, & Calleja, 2003; Sogawa, Kodama, Matsuda, Shigeta, & Okutani, 1998). The increase of sulfation level can lead to higher bioactivity (Damonte, Matulewicz, & Cerezo, 2004; Ghosh et al., 2009), therefore, the EPSs with different sulfate contents were obtained in this research by varying MgSO₄ concentration in the GYP medium (de Jesus Raposo, de Morais, & de Morais, 2014). It was found that the increase of MgSO₄·7H₂O concentration from 5.4 to 16.2 g/L in the medium increased the sulfate content of the ori EPSs, but caused only slight sulfate increase in the mut EPSs (Table 1).

The profile of constituent monosaccharides of T. striatum EPSs is simple. Only four sugars including two aldohexoses (i.e., glucose and galactose) and two pentoses (i.e., xylose and arabinose) were detected by HPLC analysis in the EPSs of both T. striatum strains (Table 1). The major monosaccharides were glucose and arabinose (up to about 90% of total carbohydrates, dry basis) followed by galactose and a small amount of xylose. Negligible mannose peaks were also found in HPLC spectra (Data not shown). The mut strain had much lower glucose, but much higher arabinose contents in its EPSs than the ori strain, which may correlate with nitrogen stress, i.e., nitrogen stress may drive the substrate carbon to synthesize more arabinose but less glucose in the EPSs of the mut strain. Overall, the sugar composition profile of the T. striatum EPSs is as simple as that of Schizochytrium genus and most microalgae (Jain et al., 2005; Xiao & Zheng, 2016) while it is different from that of the cyanobacteria EPSs which could consist of 6-12 monosaccharides (Pereira et al., 2009). In addition, the presence of ribose in the EPSs is unique among cyanobacteria, but cyanobacteria EPSs may lack arabinose and/or galactose (Parikh & Madamwar, 2006).

The molecular weight of EPSs was reported to affect their bioactivities, e.g., low molecular weight can stimulate the proliferation of macrophages and the production of NO which is involved in human immune system response (i.e., the activity strength increased with the decrease of EPS molecular weight) (Sun, Wang, Shi, & Ma, 2009; Sun, Wang, & Zhou, 2012). Therefore, we also measured the EPS molecular weight of T. striatum strains. As shown in Table 1, varying MgSO₄ concentration in the medium didn't lead to significant change of the molecular weight of the ori EPSs, however, the molecular weight of the mut EPSs increased by 2.6 and 2.5 folds with MgSO₄·7H₂O being increased from 5.4 to 10.8 and 16.2 g/L, respectively. The molecular weights of the mut EPSs were higher than that of the ori EPSs at the same MgSO₄·7H₂O concentration except for 5.4 g/L of MgSO₄·7H₂O at which the ori EPS molecular weight was more than 2 folds of the mut EPS molecular weight. This finding could be visually indicated by the AFM images that showed the ori EPSs had larger molecules than the mut EPSs (Fig. S1). The PDI value reflects the distribution of molecular weight. All EPSs had high values for PDI (e.g., > 3.5), indicating that the molecular weight distribution of EPSs was broad. The concentration of MgSO₄·7H₂O had significant effect on the PDI of the EPSs, i.e., high MgSO₄·7H₂O concentration led to high PDI for mut EPSs while 10.8 g/L MgSO₄·7H₂O achieved the highest PDI of ori EPSs. As a result, the effects of sulfate content and molecular weight on bioactivities of EPSs were analyzed in the Sections 3.2-3.5.

3.2. Structural characteristics of EPSs

The FTIR spectra of EPSs from both ori and mut strains had similar shape, but difference in absorbance intensity, indicating that there was little variation in the composition but significant variation in quantity of each individual component (Fig. 1). The big peak at 3305 cm⁻¹ was due to the bending and stretching of O–H bond in the hydroxyl functional groups (Wang, Wu, & Tang, 2009). The small peaks in the range of 2970–2850 cm⁻¹ (C–H stretching vibration) revealed a low level of lipids in ori and mut EPSs (Forfang, Zimmermann, Kosa, Kohler, & Shapaval, 2017; Jiao et al., 2010; Zhu et al., 2012) while the ori strain had a slightly bigger lipid peak for its EPSs than the mut strain. Strong amide group peaks (I & II) appeared at 1653 and 1550 cm⁻¹,

respectively (Wang et al., 2009; Zhu et al., 2012), indicating the protein as one of major components of EPSs. The two small peaks at 1465 and 1418 cm⁻¹ represented methyl group and carboxylic groups respectively, and the carboxylic groups may attribute to uronic acid (Tesson, Gaillard, & Martin-Jézéquel, 2008). It was also shown that the ori EPSs had higher peak intensities for protein and uronic acid than the mut EPSs. A large absorbance peak between 1038 and 900 cm⁻¹ indicated the existence of carbohydrates in EPSs (Zhu et al., 2012). Two small shoulders at 1126 and 970 cm⁻¹ were ascribed to sulfate groups (S=O and C-O-S bonds) in EPSs (Contreras, Sugita, & Ramos, 2006). The FTIR spectrum of taurine, a sulfur-containing β-amino acid from red algae Porphyra vezoensis also showed these sulfur peaks (Wang et al., 2015). Such sulfate groups were believed to render the EPSs of microalga Graesiella sp. antioxidant capacity (Trabelsi, Chaieb, Mnari, Abid-Essafi, & Aleya, 2016). The information shown by FTIR (Fig. 1) and Table 1 is consistent with each other in terms of composition and relative content (ori vs. mut strain) of different components in the EPSs. For instance, the ori EPSs had higher protein but lower carbohydrate contents than the mut EPSs, which was reflected by the fact that the ori EPSs had higher protein but lower carbohydrate peak intensities than the mut EPSs.

NMR analysis including ¹H, ¹³C and 2D HSQC in this study allowed us to determine the configuration of carbohydrates and most of the linkages in the polysaccharides. The ¹³C NMR spectra of the EPSs showed that the ori EPSs had a very similar polysaccharide structure to the mut EPSs (Fig. 2). The spectra revealed that the EPS comprised of a variety of components and functional groups including carbohydrates, carbonyl, carboxyl, peptide, N-containing groups, etc. The presence of polysaccharides repeating units containing Glc (glucose), Gal (galactose) and Ara (arabinose) was further assigned in the 2D HSQC spectra (Fig. 3). By comparing the contour size of anomeric carbons, stronger signals of Glc units were observed in the ori EPSs whereas the signals of Ara units were much stronger in the mut EPSs than the ori EPSs. As shown in Fig. S2, the ori EPSs had a small amount of C1 (anomeric carbon) of xylose whereas the mut EPSs did not have it. These results are in agreement with our chemical composition analysis in Table 1. The major structural linkages of the carbohydrates in both EPSs were deduced to be $1 \rightarrow 6-\beta$ -glucan and $1 \rightarrow 4-\alpha$ -galactan branched with L-α-arabinose according to the HSQC NMR chemical shifts assigned in published literature (Gharzouli et al., 2013; Lowman et al., 2011). Due to the complex compositions of EPS (i.e., several types of saccharide and protein residues), a few other cross peaks likely from carbohydrate derivatives, lipids, and protein related compounds have not been identified (black peaks in Fig. 3). We speculate that protein and carbohydrate chemically attached to each other in the EPSs because ethanol or acetone can't separate carbohydrate or protein, respectively while LC-MS failed to separate carbohydrate from protein (Data not shown) (Fig. S1). To achieve a complete assignment of peaks and linkages, we would need to find other ways to further purify the EPSs prior to the NMR analysis in our future work.

3.3. Anti-tumor activity

Uncontrolled proliferation is a key feature of malignant tumors. Anti-tumor cytotoxicity of EPS samples was determined against multiple cancer cell lines in vitro. Cytotoxicity assay of EPS samples from both ori and mut strains was first performed on B16 and DU-145 carcinoma cells. As shown in Fig. 4a and b, the ori EPSs exhibited stronger anti-tumor cytotoxicity than the mut EPSs with dose-dependent effect. In the treatment of B16 cells, $0.1\,\mu\text{g/mL}$ ori EPSs did not inhibit cell proliferation whereas significant cell death was observed when the concentration of the ori EPSs increased to $1\,\mu\text{g/mL}$ and higher dose. It was found that 1 and $10\,\mu\text{g/mL}$ didn't show significant difference, and $100\,\mu\text{g/mL}$ achieved the strongest inhibition effect (Fig. 4a). Compared to B16 cells, the ori EPSs showed stronger anti-cell proliferation activity on DU145 cells, i.e., the concentrations of 0.1 and $1\,\mu\text{g/mL}$ achieved

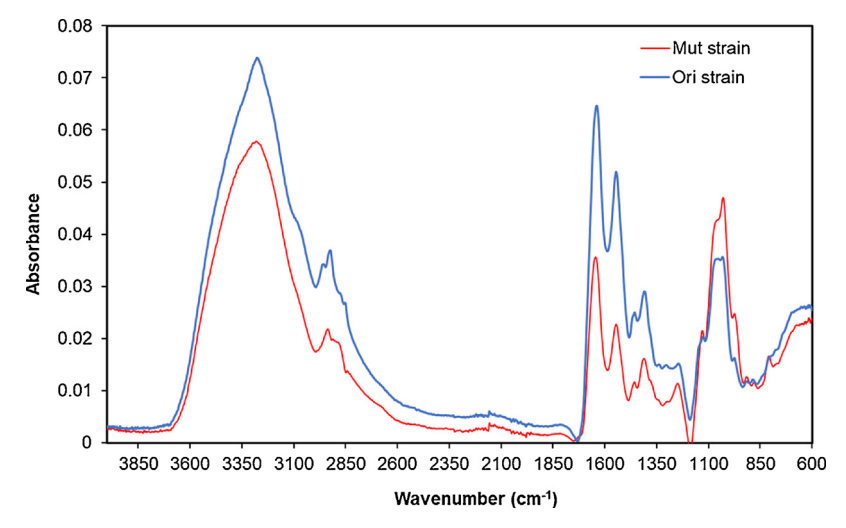


Fig. 1. FTIR spectra of the EPSs from both ori and mut strains of T. striatum with 5.4 g/L MgSO₄·7H₂O in the growth medium.

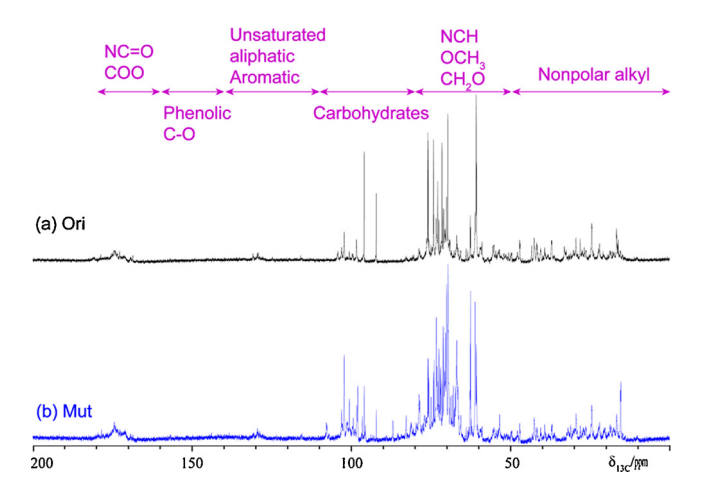


Fig. 2. 13 C NMR spectra of the EPSs from both ori (a) and mut (b) strains of *T. striatum* with 5.4 g/L MgSO₄·7H₂O in the growth medium.

similar significant inhibition on DU145 cells while increasing concentrations to 10 or $100\,\mu g/mL$ resulted in significantly further inhibition (Fig. 4b). In contrast, the mut EPSs did not show significant inhibition effect on B16 or DU145 cells until their concentration reached $100\,\mu g/mL$ (Fig. 4a and b). In the study of cytotoxicity on NL20 non-tumorigenesis epithelial cells, neither the ori nor mut EPSs was found to significantly inhibit NL20 cells until their concentrations reached $100\,\mu g/mL$ (Fig. 4c).

In addition to B16 and DU145 cells, another batch of anti-tumor activity assay was conducted on A549 lung carcinoma and HeLa cervical carcinoma cell lines by using both ori and mut EPSs that were obtained from T. striatum cultures grown in the medium with various MgSO₄·7H₂O concentrations (i.e., 5.4, 10.8 and 16.2 g/L). In the tested dose range (0.1-100 $\mu g/mL$), all EPS samples except for the ori EPS sample with $5.4\,g/L$ of $MgSO_4.7H_2O$ (ori $5.4_0.1$ -ori 5.4_100) in the cultivation medium had significant effect on the inhibition of A549 cells at the EPS concentration of $100 \,\mu g/mL$ (Fig. 5a). It was also found that the ori and mut EPSs with the same MgSO₄·7H₂O concentration had similar anti-tumor activity on A549 cells at the same dose level except for the EPSs with 5.4 g/L of MgSO₄·7H₂O. As for HeLa cells, the ori EPSs **EPSs** excluding the with $16.2 \, g/L$ of MgSO₄·7H₂O

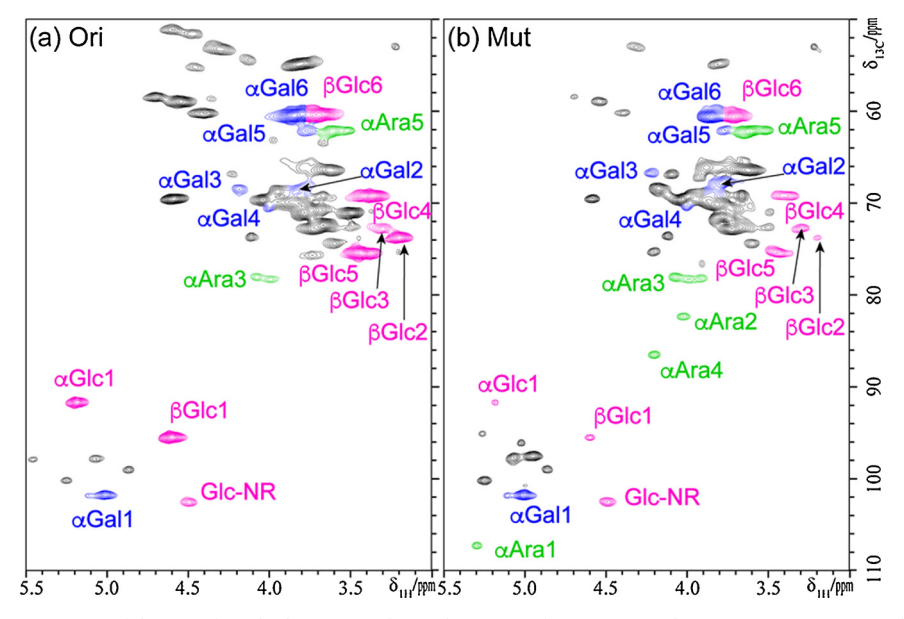
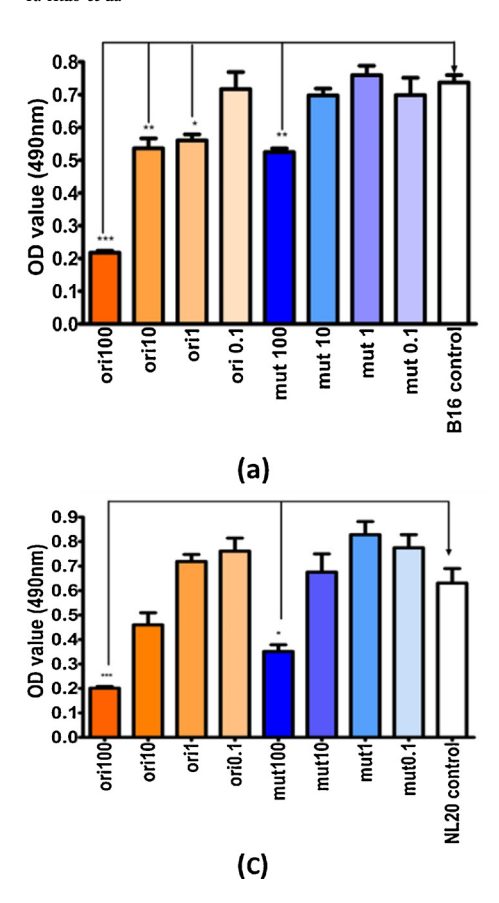


Fig. 3. ¹³C-1H HSQC short range spectra of the EPSs from both ori (a) and mut (b) strains of *T. striatum* with 5.4 g/L MgSO₄·7H₂O in the growth medium revealing carbohydrates units and linkages.



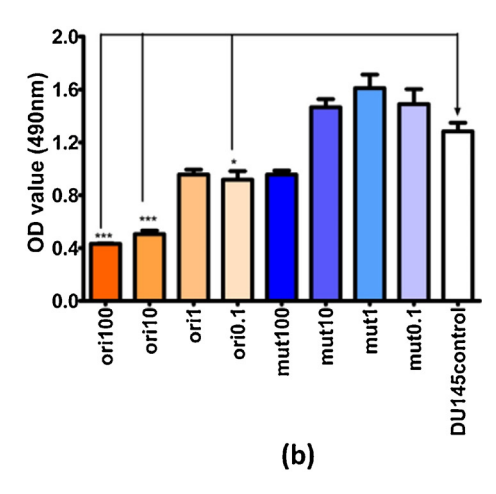
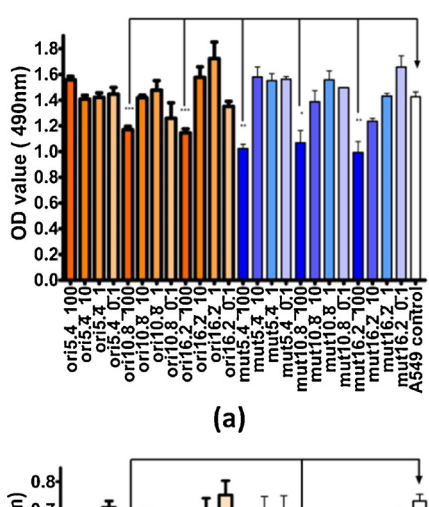
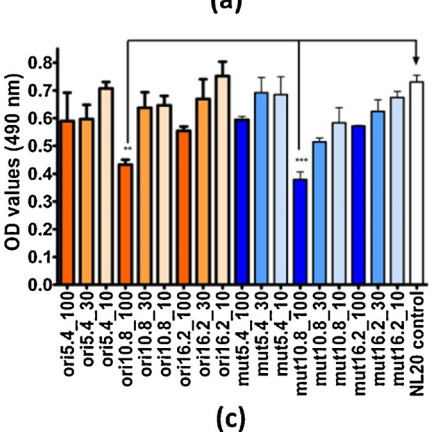


Fig. 4. MTS cytotoxicity assay of EPS samples on B16 melanoma (a), DU145 prostate carcinoma (b) and NL20 lung epithelial cells (c). All EPS samples were obtained from the T. striatum cultures grown in the medium with 5.4 g/L of MgSO₄·7H₂O. The ori EPS samples are coded in orange (labeled as "ori") and the mut EPS samples are coded in blue (labeled as "mut"). The numbers (0.1-100) in the labels denote EPS concentrations in $\mu g/mL$. The Ep statistical differences were determined between the treatment and the no-treatment control bars (***p < 0.001, **p < 0.01 and *p < 0.05).(For interpretation of the references to color in this figure legend, the reader is referred to the web version of this article.)





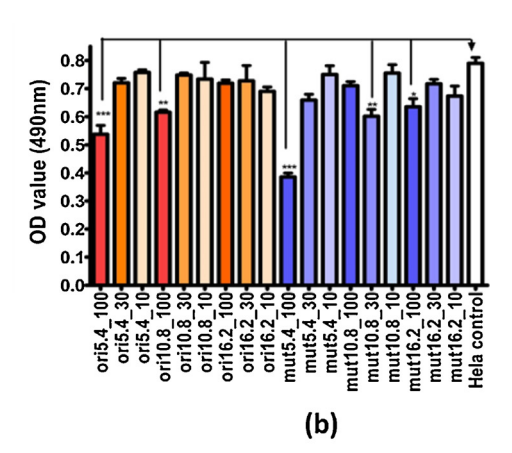


Fig. 5. MTS cytotoxicity assay of EPS samples on A549 lung carcinoma (a), HeLa cervical carcinoma (b) and NL20 lung epithelial cells (c). The ori EPS samples are coded in orange (labeled as "ori") and the mut EPS samples are coded in blue (labeled as "mut"). EPS samples were obtained from cultures grown in medium with different MgSO₄·7H₂O concentrations (5.4, 10.8 and 16.2 g/L) as labeled. The numbers (10, 30 and 100) in the labels denote EPS concentrations in µg/mL. The Ep statistical differences were determined between the treatment and the no-treatment control bars (***p < 0.001, **p < 0.01 and *p < 0.05).(For interpretation of the references to color in this figure legend, the reader is referred to the web version of this article.)

(ori16.2_10-ori16.2_100) had significant inhibitions on cancer cells at 100 µg/mL (Fig. 5b). However, the mut EPSs with three levels of MgSO₄·7H₂O (5.4, 10.8 and 16.2 g/L) inhibited HeLa cells significantly at 100, 30 and 100 µg/mL, respectively (Fig. 5b). Overall, the dose of EPSs was a critical factor affecting their anti-tumor activity on A549 and HeLa cells, while MgSO₄ concentration did not show significant effect on the anti-tumor activity of EPSs on both cancer cells. MTS assay was also conducted on NL20 non-tumorigenesis epithelial to demonstrate if EPS samples were able to target tumor cells selectively while sparing normal cells/tissues (Fig. 5c). The ori and mut EPSs had similar anti-tumor selectivity under the same conditions. For the EPSs produced with the same MgSO₄ concentration in the medium, the increasing EPS dose reduced the selectivity. Among all the tested EPSs. only the ori and mut EPSs with 10.8 g/L of MgSO₄·7H₂O (ori10.8_100 and mut10.8_100) inhibited NL20 cells significantly at the dose of 100 µg/mL, i.e., their selectivity was the lowest. By analyzing Fig. 5 against Table 1, the sulfate content and molecular weight of the EPSs did not appear to affect anti-tumor activities on B16 and DU145 cells.

3.4. Antioxidant activity

As oxidative stress contributes to the development of many diseases including cancer, Alzheimer's disease, Parkinson's disease and neurodegeneration, the use of antioxidants in pharmacology has been intensively studied (Nishino et al., 2004). The trolox equivalent total antioxidant capacity (TAC) of various EPS samples was measured to reflect the TAC of EPS samples (Fig. 6). The higher trolox equivalent amount represented better antioxidant capacity. The results demonstrated that both ori and mut EPS samples yielded promising TAC at 100 µg/mL. To determine the TAC of EPSs at lower dose between 10 and 100 µg/mL, the same assay was repeated at the concentration of 30 µg/mL for the top three EPS samples (ori5.4, ori10.8 and mut5.4) which achieved the best TAC at 100 μg/mL. It was found the 30 μg/mL did not result in significant increase of TAC compared with 10 µg/mL (data not shown). These results indicated that the applied EPS dose was of more importance while the sulfate content and molecular weight of EPSs seemed insignificant in affecting the TAC values.

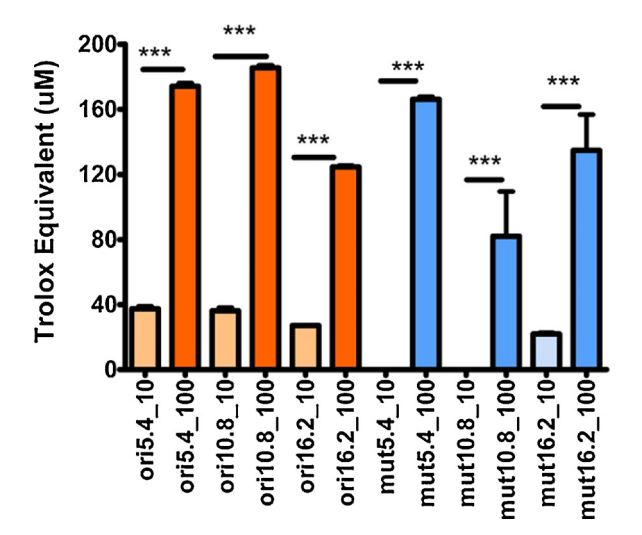


Fig. 6. Total antioxidant capacity (TAC) of EPSs. The ori EPSs are coded in orange (labeled as "ori") and the mut EPSs are coded in blue (labeled as "mut"). The numbers (5.4, 10.8 and 16.2) in the labels are MgSO₄·7H₂O concentration (g/L) in the GYP medium, and 10 and 100 denote the dose of EPSs at 10 and 100 µg/mL, respectively. The Ep statistical differences were determined between the doses of each EPS samples (***p < 0.001). (For interpretation of the references to color in this figure legend, the reader is referred to the web version of this article.)

3.5. Anti-inflammatory activity

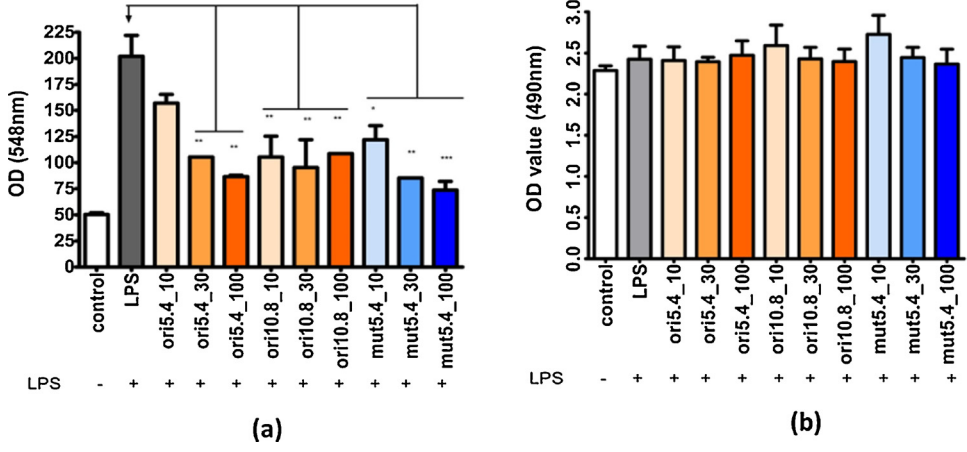
Inflammation plays an important role in the evolution of cancer (Coussens & Werb, 2002) and many other diseases. Specifically, sustained production of NO endows macrophages with cytostatic or cytotoxic activity against viruses, bacteria, fungi, protozoa, and tumor cells (MacMicking, Xie, & Nathan, 1997). NO-based anti-inflammation test was performed on macrophage cells (Raw 264.7) to examine if EPSs exerted anti-inflammation activity. In our experiment, LPS was utilized to induce inflammation on macrophages. The results indicated that all tested EPSs possessed the anti-inflammation ability by significantly decreasing the NO production (Fig. 7a). To rule out the possibility that decreased NO production was caused by the EPS-induced cell death, the cell proliferation assay was also performed. The results demonstrated that the EPS treatment did not affect macrophage cell proliferation (Fig. 7b), which means it was the anti-inflammatory activity of EPS that reduced the NO production. It can be also seen that the ori and mut EPSs did not have significant difference on anti-inflammatory activity, and the dose-effect (except for the 10 µg/mL of the EPSs obtained at 5.4 g/L of MgSO₄·7H₂O) was insignificant in the testing range (Fig. 7a). Only two levels of sulfate contents and molecular weight of EPSs were analyzed for the ori EPSs (obtained with 5.4 and 10.8 g/L of MgSO₄·7H₂O), and no significant difference was found between them.

3.6. Antibacterial activity

A list of Gram⁺ and Gram⁻ bacterial pathogens were selected to test the antibacterial activity of the EPSs. The ZOI assays were used as an initial screening of EPS-sensitive bacteria. Of the bacteria tested, only P. aeruginosa was found sensitive to both the ori and mut EPSs, as indicated by a large clear zone around the EPS-impregnated filter disc (Fig. 8). The dose of the EPSs had a significant effect on ZOI (i.e., the diameter was enlarged with the increase of the EPS concentration) (Table 2). In addition, the ori and mut EPSs showed similar ZOI results at the tested concentrations except for 1 mg/mL at which 22 mm ZOI of the mut EPSs was achieved in contrast to the 0 mm ZOI of the ori EPSs. We further tested the minimal inhibition concentration (MIC) of the EPSs on P. aeruginosa. However, no inhibition was observed even with the highest concentration of EPS used (i.e., 10 mg/mL). Maybe the EPS is not stable when dissolved in LB broth. More research will be conducted to figure out the reasons for the difference between ZOI and MIC tests.

4. Conclusions

Through the comparison between the ori and mut strains, it was found that the nitrogen stress can induce strain alternation, which was conducive for EPS production of T. striatum while enhancing the polysaccharide and reducing protein contents in the EPSs. Meanwhile, such nitrogen stress also altered the monosaccharide profile of the polysaccharide in the EPSs by reducing glucose while increasing arabinose content. Increasing sulfate concentration in the cultivation medium significantly increased the EPS yield of both strains and the molecular weight of the mut EPSs, but slightly altered the compositions of the EPSs. FTIR mainly indicated the characteristic functional groups of polysaccharide and protein of EPSs associated with small amount of uronic acid, sulfate and lipid. NMR effectively detected the major structural linkages of the polysaccharides of the EPSs which was $1 \rightarrow 6$ β-glucan and 1 \rightarrow 4- α -galactan branched with L- α -arabinose. It was also deduced that protein is chemically connected with polysaccharide in the EPSs. The bioactivity assay demonstrated that the EPSs from both the ori and mut strains are promising bioactive compounds with antitumor, antioxidant, anti-inflammatory, and antibacterial activities. Both reliefs of oxidative stress and inflammation suppression are important factors among cancer treatment strategies. The ori and mut EPSs did not show significance difference in the tested bioactivities



legend, the reader is referred to the web version of this article.)

Fig. 7. Anti-inflammation test on macrophage Raw 264.7 cells. (a) NO measurement was performed using Griess reagent kit (Molecular Probes), and (b) MTS assay was performed to evaluate the cell proliferation. The ori EPS samples are coded in orange (labeled as "ori") and the mut EPS samples are coded in blue (labeled as "mut"). The blank and LPS controls are coded in white and grey, respectively. The numbers (5.4, 10.8 and 16.2) in the labels are MgSO₄·7H₂O concentration (g/L) in the growth medium for T. striatum, and 10, 30 and 100 denote the dose of EPSs at 10, 30 and 100 µg/ mL, respectively. The Ep statistical differences were determined between the treatment and the LPS control bars (***p < 0.001, **p < 0.01 and *p < 0.05). (For interpretation of the references to color in this figure

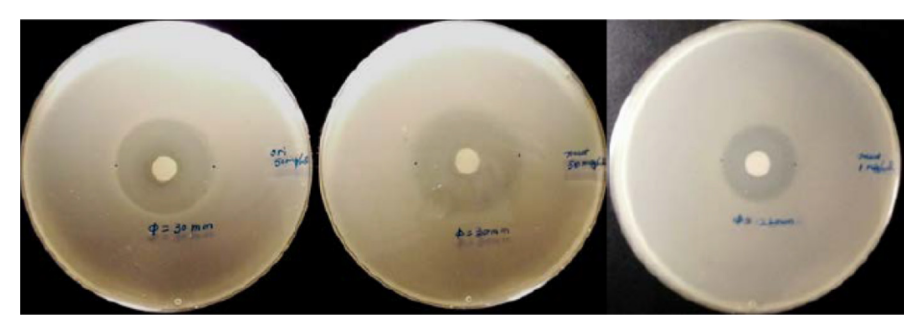


Fig. 8. Example ZOI of EPSs on *P. aeruginosa*. Left: the ori EPSs at 50 mg/mL; and middle and right: the mut EPSs at 50 mg/mL and 1 mg/mL, respectively. All tested EPSs here were obtained with 5.4 g/L MgSO₄·7H₂O in GYP medium.

Table 2 Diameters of the inhibition zones.

EPS concentration (mg/mL)	Ori strain (mm)	Mut strain (mm)
50	30	30
20	25	25
10	22	22
1	0	22

except that the mut EPSs were more effective in inhibiting P. aeruginosa than the ori EPSs. The EPSs from T. striatum are a promising new class of marine biopharmaceuticals with multiple important bioactivities, which would promote the research on the development of marine protist-based biopharma.

Acknowledgements

The authors would like to thank Drs. David Ladner and Brian Powell, Associate Professors in the Department of Environmental Engineering and Earth Sciences, Clemson University for their help with EPS separation and FTIR analysis, respectively. The authors' gratitude also goes to Prof. Igor Luzinov and Dr. Ruslan Burtovyy (Postdoctoral Researcher) in the Department of Materials Science and Engineering, Clemson University for their help with AFM imaging. The authors appreciate the undergraduate Creative Inquiry (CI) group in Dr. Wei's lab for conducting the anti-tumor, antioxidant, and anti-inflammatory assays. The research was partially supported by Clemson University's CI fund. This research did not receive any specific grant from funding agencies in the public, commercial, or not-for-profit sectors.

Appendix A. Supplementary data

Supplementary data associated with this article can be found, in the

online version, at https://doi.org/10.1016/j.carbpol.2018.04.126.

References

Aki, T., Hachida, K., Yoshinaga, M., Katai, Y., Yamasaki, T., Kawamoto, S., et al. (2003). Thraustochytrid as a potential source of carotenoids. *Journal of the American Oil Chemists' Society*, 80, 789–794.

Arad, S., & Atar, D. (2015). Viscosupplementation with algal polysaccharides in the treatment of arthritis. Google Patents.

Arad, S., Rapoport, L., Moshkovich, A., van Moppes, D., Karpasas, M., Golan, R., et al. (2006). Superior biolubricant from a species of red microalga. *Langmuir*, 22(17), 7313–7317.

Bender, J., & Phillips, P. (2004). Microbial mats for multiple applications in aquaculture and bioremediation. *Bioresource Technology*, *94*(3), 229–238.

Bongiorni, L., Jain, R., Raghukumar, S., & Aggarwal, R. R. (2005). *Thraustochytrium gaertnerium* sp. nov.: A new thraustochytrid stramenopilan protist from Mangroves of Goa, India. *Protist*, *156*, 303–315.

Burja, A. M., Radianingtyas, H., Windust, A., & Barrow, C. J. (2006). Isolation and characterization of polyunsaturated fatty acid producing Thraustochytrium species: Screening of strains and optimization of omega-3 production. Applied Microbiology and Biotechnology, 72(6), 1161.

Burja, A. M., Armenta, R. E., Radianingtyas, H., & Barrow, C. J. (2007). Evaluation of fatty acid extraction methods for Thraustochytrium sp. ONC-T18. *Journal of Agricultural and Food Chemistry*, 55(12), 4795–4801.

Byreddy, A., Gupta, A., Barrow, C., & Puri, M. (2015). Comparison of cell disruption methods for improving lipid extraction from thraustochytrid strains. *Marine Drugs*, 13(8), 5111.

Byreddy, A. R. (2016). Thraustochytrids as an alternative source of omega-3 fatty acids, carotenoids and enzymes. *Lipid Technology*, 28(3–4), 68–70.

Carmona, M. L., Naganuma, T., & Yamaoka, Y. (2003). Identification by HPLC-MS of carotenoids of the Thraustochytrium CHN-1 strain isolated from the Seto Inland Sea Bioscience, Biotechnology, and Biochemistry, 67(4), 884–888.

Chi, Z., Su, C. D., & Lu, W. D. (2007). A new exopolysaccharide produced by marine Cyanothece sp. 113. Bioresource Technology, 98(6), 1329–1332.

Contreras, C., Sugita, S., & Ramos, E. (2006). Preparation of sodium aluminate from basic aluminum sulfate. Advances in Technology of Materials and Materials Processing Journal, 8(2), 122.

Coussens, L. M., & Werb, Z. (2002). Inflammation and cancer. *Nature*, 420, 860. Damonte, E. B., Matulewicz, M. C., & Cerezo, A. S. (2004). Sulfated seaweed polysaccharides as antiviral agents. *Current Medicinal Chemistry*, 11(18), 2399–2419.

de Jesus Raposo, M. F., de Morais, R. M. S. C., & Bernardo de Morais, A. M. M. B. (2013). Bioactivity and applications of sulphated polysaccharides from marine microalgae.

- Marine Drugs, 11(1), 233.
- de Jesus Raposo, M. F., de Morais, A. M. M. B., & de Morais, R. M. S. C. (2014). Influence of sulphate on the composition and antibacterial and antiviral properties of the exopolysaccharide from Porphyridium cruentum. *Life Sciences*, 101(1), 56–63.
- de Jesus Raposo, M. F., de Morais, A. M. M. B., & de Morais, R. M. S. C. (2015a). Marine polysaccharides from algae with potential biomedical applications. *Marine Drugs*, 13(5), 2967.
- de Jesus Raposo, M. F., de Morais, A. M. M. B., & de Morais, R. M. S. C. (2015b). Bioactivity and applications of polysaccharides from marine microalgae. Polysaccharides: Bioactivity and biotechnology1683–1727.
- Decho, A. W. (1990). Microbial exopolymer secretions in ocean environments: Their role (s) in food webs and marine processes. Oceanogr. Mar. Biol. Annu. Rev. 28(7), 73–153.
- Dodgson, K. S. (1961). Determination of inorganic sulphate in studies on the enzymic and non-enzymic hydrolysis of carbohydrate and other sulphate esters. *Biochemical Journal*, 78(2), 312–319.
- Fabregas, J., García, D., Fernandez-Alonso, M., Rocha, A. I., Gómez-Puertas, P., Escribano, J. M., et al. (1999). In vitro inhibition of the replication of haemorrhagic septicaemia virus (VHSV) and African swine fever virus (ASFV) by extracts from marine microalgae. Antiviral Research, 44, 67–73.
- Fan, K. W., Vrijmoed, L. L. P., & Jones, E. B. G. (2002). Physiological studies of subtropical mangrove Thraustochytrids. Botanica Marina, 45, 50–57.
- Flemming, H.-C., & Wingender, J. (2010). The biofilm matrix. Nature Reviews Microbiology, 8, 623.
- Forfang, K., Zimmermann, B., Kosa, G., Kohler, A., & Shapaval, V. (2017). FTIR spectroscopy for evaluation and monitoring of lipid extraction efficiency for oleaginous fungi. PLoS One, 12(1), e0170611. http://dx.doi.org/10.1371/journal.pone. 0170611
- Gasljevic, K., Hall, K., Chapman, D., & Matthys, E. F. (2008). Drag-reducing polysaccharides from marine microalgae: Species productivity and drag reduction effectiveness. *Journal of Applied Phycology*, 20(3), 299–310.
- Geresh, S., Dubinsky, O., Arad, S., Christiaen, D., & Glaser, R. (1990). Structure of 3-O-(α-d-glucopyranosyluronic acid)-l-galactopyranose, an aldobiouronic acid isolated from the polysaccharides of various unicellular red algae. Carbohydrate Research, 208, 301–305.
- Geresh, S., Arad, S., & Shefer, A. (1997). Chemically crosslinked polysaccharide of the red microalga Rhodella reticulata–An ion exchanger for toxic metal ions. *Journal of Carbohydrate Chemistry*. 16(4-5), 703–708.
- Gharzouli, R., Carpéné, M.-A., Couderc, F., Benguedouar, A., & Poinsot, V. (2013).
 Relevance of fucose-rich extracellular polysaccharides produced by Rhizobium sullae strains nodulating hedysarum Coronarium L. legumes. Applied and Environmental Microbiology. 79(6). 1764–1776.
- Ghosh, T., Chattopadhyay, K., Marschall, M., Karmakar, P., Mandal, P., & Ray, B. (2009). Focus on antivirally active sulfated polysaccharides: From structure–activity analysis to clinical evaluation. *Glycobiology*, *19*(1), 2–15.
- Guzmán, S., Gato, A., Lamela, M., Freire-Garabal, M., & Calleja, J. M. (2003). Anti-in-flammatory and immunomodulatory activities of polysaccharide from Chlorella stigmatophora and Phaeodactylum tricornutum. *Phytotherapy Research*, 17(6), 665–670.
- Ha, Y. W., Dyck, L. A., & Thomas, R. L. (1988). Hydrocolloids from the freshwater microalgae, Palmella texensis and Cosmarium turpinii. *Journal of Food Science*, 53(3), 841–844.
- Harrison, J. L., & Jones, E. B. G. (1974). Zoospore discharge in Thraustochytrium striatum. Transactions of the British Mycological Society, 62, 283–288.
- Jain, R., Raghukumar, S., Tharanathan, R., & Bhosle, N. B. (2005). Extracellular polysaccharide production by thraustochytrid protists. *Marine Biotechnology*, 7(3), 184–192.
- Jiao, Y., Cody, G. D., Harding, A. K., Wilmes, P., Schrenk, M., Wheeler, K. E., et al. (2010). Characterization of extracellular polymeric substances from acidophilic microbial biofilms. Applied and Environmental Microbiology, 76, 2916–2922.
- Lee Chang, K. J., Nichols, C. M., Blackburn, S. I., Dunstan, G. A., Koutoulis, A., & Nichols, P. D. (2014). Comparison of Thraustochytrids Aurantiochytrium sp., Schizochytrium sp., Thraustochytrium sp., and Ulkenia sp. for production of biodiesel, long-chain omega-3 oils, and exopolysaccharide. *Marine Biotechnology*, 16(4), 396–411.
- Liu, Y., Singh, P., Sun, Y., Luan, S., & Wang, G. (2014). Culturable diversity and biochemical features of thraustochytrids from coastal waters of Southern China. Applied Microbiology and Biotechnology, 98(7), 3241–3255.
- Lowman, D. W., West, L. J., Bearden, D. W., Wempe, M. F., Power, T. D., Ensley, H. E., et al. (2011). New insights into the structure of $(1 \rightarrow 3, 1 \rightarrow 6)$ - β -D-glucan side chains in the Candida glabrata cell wall. *PLoS One*, 6, e27614. http://dx.doi.org/10.1371/journal.pone.0027614.
- MacMicking, J., Xie, Q. W., & Nathan, C. (1997). Nitric oxide and macrophage function. Annual Review of Immunology, 15, 323–350.
- Masuko, T., Minami, A., Iwasaki, N., Majima, T., Nishimura, S.-I., & Lee, Y. C. (2005). Carbohydrate analysis by a phenol-sulfuric acid method in microplate format. *Analytical Biochemistry*, 339(1), 69–72.

- Mishra, A., & Jha, B. (2009). Isolation and characterization of extracellular polymeric substances from micro-algae Dunaliella salina under salt stress. *Bioresource Technology*, 100(13), 3382–3386.
- Mojica, K., Elsey, D., & Cooney, M. J. (2007). Quantitative analysis of biofilm EPS uronic acid content. *Journal of Microbiological Methods*, 71(1), 61–65.
- Nagano, N., Taoka, Y., Honda, D., & Hayashi, M. (2009). Optimization of culture conditions for growth and docosahexaenoic acid production by a marine thraustochytrid, Aurantiochytrium limacinum mh0186. *Journal of Oleo Science*, 58(12), 623–628.
- Nie, X.-N., Liu, J., She, D., Sun, R.-C., & Xu, F. (2013). Physicochemical and structural characterization of hemicelluloses isolated by different alcohols from rice straw.
- Nishino, H., Tokuda, H., Satomi, Y., Masuda, M., Osaka, Y., Yogosawa, S., et al. (2004). Cancer prevention by antioxidants. *Biofactors*, 22(1–4), 57–61.
- Parikh, A., & Madamwar, D. (2006). Partial characterization of extracellular polysaccharides from cyanobacteria. Bioresource Technology, 97(15), 1822–1827.
- Pereira, S., Zille, A., Micheletti, E., Moradas-Ferreira, P., De Philippis, R., & Tamagnini, P. (2009). Complexity of cyanobacterial exopolysaccharides: Composition, structures, inducing factors and putative genes involved in their biosynthesis and assembly. FEMS Microbiology Reviews, 33(5), 917–941.
- Raghukumar, S., & Raghukumar, C. (1999). Thraustochytrid fungoid protists in faecal pellets of the tunicate Pegea confoederata, their tolerance to deep-sea conditions and implication in degradation processes. *Marine Ecology Progress Series*, 190, 133–140.
- Raghukumar, S., Sharma, S., Raghukumar, C., Sathe-Pathak, V., & Chandramohan, D. (1994). Thraustochytrid and fungal component of marine detritus. IV. Laboratory studies on decomposition of leaves of the mangrove Rhizophora apiculata Blume. Journal of Experimental Marine Biology and Ecology, 183, 113–131.
- Raghukumar, S., Sathe-Pathak, V., Sharma, S., & Raghukumar, C. (1995). Thraustochytrid and fungal component of marine detritus. III. Field studies on decomposition of leaves of the mangrove *Rhizophora apiculata*. Aquatic Microbial Ecology, 9, 117–125.
- Raghukumar, S., Anil, A. C., Khandeparker, L., & Patil, J. S. (2000). Thraustochytrid protists as a component of marine microbial films. *Marine Biology*, 136(4), 603–609.
- Raghukumar, S. (1992). Bacterivory: A novel dual role for thraustochytrids in the sea. Marine Biology, 113, 165–169.
- Raghukumar, S. (2002). Ecology of the marine protists, the Labyrinthulomycetes (Thraustochytrids and Labyrinthulids). European Journal of Protistology, 38(2), 127–145.
- Singh, D., Gupta, A., Wilkens, S. L., Mathur, A. S., Tuli, D. K., Barrow, C. J., et al. (2015). Understanding response surface optimisation to the modeling of Astaxanthin extraction from a novel strain Thraustochytrium sp. S7. *Algal Research*, 11, 113–120.
- Sluiter, A., Hames, B., Ruiz, R., Scarlata, C., Sluiter, J., Templeton, D., et al. (2008). Determination of structural carbohydrates and lignin in biomass. http://www.nrel.gov/docs/gen/fy13/42618.pdf. (Accessed 10 September 2017).
- Sogawa, K., Kodama, E., Matsuda, M., Shigeta, S., & Okutani, K. (1998). Marine microalgal polysaccharide induces apoptosis in human lymphoid cells. *Journal of Marine Biotechnology*, 6, 35–38.
- Sun, L., Wang, C., Shi, Q., & Ma, C. (2009). Preparation of different molecular weight polysaccharides from Porphyridium cruentum and their antioxidant activities. *International Journal of Biological Macromolecules*, 45(1), 42–47.
- Sun, L., Wang, L., & Zhou, Y. (2012). Immunomodulation and antitumor activities of different-molecular-weight polysaccharides from Porphyridium cruentum. *Carbohydrate Polymers*, 87(2), 1206–1210.
- Sutherland, I. W. (1998). Novel and established applications of microbial polysaccharides. *Trends in Biotechnology*, 16(1), 41–46.
- Taoka, Y., Nagano, N., Okita, Y., Izumida, H., Sugimoto, S., & Hayashi, M. (2009).
 Extracellular enzymes produced by marine eukaryotes, *Thraustochytrids. Bioscience*, *Biotechnology, and Biochemistry*, 73, 180–182.
- Tesson, B., Gaillard, C., & Martin-Jézéquel, V. (2008). Brucite formation mediated by the diatom Phaeodactylum tricornutum. *Marine Chemistry*, 109(1), 60–76.
- Trabelsi, L., Chaieb, O., Mnari, A., Abid-Essafi, S., & Aleya, L. (2016). Partial characterization and antioxidant and antiproliferative activities of the aqueous extracellular polysaccharides from the thermophilic microalgae Graesiella sp. BMC Complementary and Alternative Medicine, 16(1), 210.
- Wang, Z., Wu, Z., & Tang, S. (2009). Extracellular polymeric substances (EPS) properties and their effects on membrane fouling in a submerged membrane bioreactor. Water Research, 43(9), 2504–2512.
- Wang, F., Guo, X.-Y., Zhang, D.-N., Wu, Y., Wu, T., & Chen, Z.-G. (2015). Ultrasound-assisted extraction and purification of taurine from the red algae Porphyra yezoensis. Ultrasonics Sonochemistry, 24, 36–42.
- Xiao, R., & Zheng, Y. (2016). Overview of microalgal extracellular polymeric substances (EPS) and their applications. Biotechnology Advances, 34(7), 1225–1244.
- Yaron, A., Cohen, E., & Arad, S. M. (1992). Stabilization of aloe vera gel by interaction with sulfated polysaccharides from red microalgae and with xanthan gum. *Journal of Agricultural and Food Chemistry*, 40(8), 1316–1320.
- Zhu, L., Qi, H.-Y., Lv, M.-L., Kong, Y., Yu, Y.-W., & Xu, X.-Y. (2012). Component analysis of extracellular polymeric substances (EPS) during aerobic sludge granulation using FTIR and 3D-EEM technologies. *Bioresource Technology*, 124, 455–459.